Quantum-Confined Stark Effect in Ge/SiGe Quantum Wells on Si for Optical Modulators

Yu-Hsuan Kuo, *Student Member, IEEE*, Yong Kyu Lee, *Member, IEEE*, Yangsi Ge, Shen Ren, Jonathan E. Roth, Theodore I. Kamins, *Fellow, IEEE*, David A. B. Miller, *Fellow, IEEE*, and James S. Harris, Jr., *Fellow, IEEE*

Abstract—We present observations of quantum confinement and quantum-confined Stark effect (QCSE) electroabsorption in Ge quantum wells with SiGe barriers grown on Si substrates, in good agreement with theoretical calculations. Though Ge is an indirect gap semiconductor, the resulting effects are at least as clear and strong as seen in typical III–V quantum well structures at similar wavelengths. We also demonstrate that the effect can be seen over the C-band around 1.55-μm wavelength in structures heated to 90 °C, similar to the operating temperature of silicon electronic chips. The physics of the effects are discussed, including the effects of strain, electron and hole confinement, and exciton binding, and the reasons why the effects should be observable at all in such an indirect gap material. This effect is very promising for practical high-speed, low-power optical modulators fabricated compatible with mainstream silicon electronic integrated circuits.

Index Terms—Electroabsorption effect, germanium, optical interconnections, optical modulators, quantum-confined Stark effect (QCSE), silicon.

I. INTRODUCTION

THE quantum-confined Stark effect (QCSE) [1], [2] is a strong, electric field dependent change in optical absorption (electroabsorption) that has been seen in quantum well materials. It is used extensively for high-speed [3], low power dissipation optical modulators, for example, in telecommunications, and has also been used in large arrays of low power devices [4]. To this point, nearly all examples of the QCSE have been in III–V semiconductor quantum wells, such as GaAs with AlGaAs barriers, or InGaAs with InP barriers. It would be very useful to make modulators with similar performance in a way that is compatible with silicon-integrated circuit manufacture. That would enable fully integrated modulators and driver circuits in silicon technology for telecommunications applications, potentially reducing costs. With suitably low-power modulators, dense optical interconnects to and from silicon electronics could be contemplated,

potentially solving severe scaling problems of electrical wiring being experienced within electronic systems today [5]–[7].

Silicon itself has only relatively weak mechanisms, such as the carrier density dependence of refractive index [8], for making modulators. Recent works, using either long waveguides with small cross sections [9], or very highly resonant structures [10] that must be precisely tuned to the operating wavelength, have demonstrated working modulators in silicon.

Demonstration of stronger mechanisms, such as the QCSE, in a silicon-compatible materials system could open up many new possibilities for modulators, avoiding long lengths or precise tuning, for example.

One possible approach would be to integrate III–V devices with silicon. Hybrid integration is quite feasible [4], though a monolithic approach might ideally be preferable to reduce costs. Substantial issues remain for the monolithic integration of III–V materials with silicon, however, not least because group III and group V materials are dopants for silicon. Germanium is, however, routinely used together with silicon in some integrated circuits [11], so the basic problems of materials compatibility between silicon and germanium in a manufacturable process have been resolved. A key question is therefore whether the use of germanium could allow strong modulation mechanisms, such as the QCSE. Germanium, like silicon, is an indirect gap semiconductor (as we will discuss in greater detail later). However, no indirect gap material has ever previously shown clear QCSE effects, despite some interesting attempts [12].

Previous efforts to find mechanisms such as the QCSE in Si/Ge structures have had limited success. SiGe/Si quantum wells with type-I alignment (electron and hole minima in the same material layer) show either no QCSE [13] or relatively inefficient effects [14], [15]. Strained SiGe/Si quantum wells on relaxed SiGe buffers [16] and Ge/Si quantum dots [17] on Si substrates, with type-II band alignment (electron and hole energy minima in different layers), can exhibit large shifts of optical transitions with the electric field, but have relatively low absorption associated with the shifting transitions.

Recently, we have briefly reported [18] strong QCSE in germanium quantum wells grown on silicon substrates with SiGe barriers. These observations show clear QCSE whose performance is comparable to, or possibly better than, III–V QCSE effects at similar wavelengths. Here, we give an extended discussion of this work, and also show that this effect can be observed in redesigned structures, operated at the kinds of temperatures encountered on the surface of the silicon complementary metal–oxide–semiconductor (CMOS) electronic chips,

Y.-H. Kuo, Y. Ge, S. Ren, J. E. Roth, D. A. B. Miller, and J. S. Harris, Jr. are with the Solid State and Photonics Laboratory, Stanford University, Stanford, CA 94305 USA (e-mail: yhkuo@snow.stanford.edu; jimbond@stanford.edu; renshen@stanford.edu; jonroth@stanford.edu; dabm@ee.stanford.edu; harris@snowmass.stanford. edu).

Y. K. Lee was with the Solid State and Photonics Laboratory, Stanford University, Stanford, CA 94305 USA. He is now with Samsung Electronics, Kyungsangbuk-do, Korea (e-mail: yklee3@samsumg.com).

T. I. Kamins is with the Solid State and Photonics Laboratory, Stanford University, Stanford, CA 94305 USA, and also with Quantum Science Research, Hewlett-Packard Laboratories, Palo Alto, CA 94304 USA (e-mail: kamins@hp.com).

Digital Object Identifier 10.1109/JSTQE.2006.883146

in the technologically important C-band around 1.55-μm wavelength, the main wavelength band used for telecommunications.

In Section II, we discuss the form of the band structure in Ge, Si, and Ge-rich SiGe, the materials used in our structures. The structure growth techniques and the optical measurement methods are described in Section III. In Section IV, we present the experimental results on two different samples. The calculation of the quantum well energies and shifts, and the sensitivity to various parameters, are presented in Section V. The physics of the QCSE in this indirect material is discussed in Section VI, and conclusions are drawn in Section VII. Exciton binding energies and shifts with field are discussed in the Appendix.

II. BAND STRUCTURE AND SAMPLE DESIGN

Both Si and Ge are indirect bandgap materials. Though the maximum in the valence band is at the zone center (zero effective momentum), the global minima in the conduction band of Si and Ge are not at the zone center. The fact that the valence band maxima and the conduction band minima are not at the same effective momentum means that the optical transitions between these maxima and minima are indirect, that is, they necessarily involve phonons so that the effective momentum can be conserved, because the photon momemtum is negligible on this scale.

As photon energy is increased from below this lowest, indirect bandgap energy (the separation between the highest valence band maximum and the lowest conduction band minimum), the optical absorption rises relatively slowly and weakly compared to that in the direct gap materials such as GaAs. In Ge, however, there is also a local minimum in the conduction band at the zone center. Thus, though Ge has a weak, indirect optical absorption tail extending almost to 2-μm wavelength ($\sim$0.62 eV) at room temperature [19], it also has a strong and abrupt rising absorption edge at $\sim$1.55-μm wavelength ($\sim$0.8 eV) [20]. This strong edge corresponds to the direct optical absorption at the zone center. The band structure of this zone center minimum and of the zone-center valence band maxima is essentially similar to that of the direct gap materials like GaAs, and is expected to behave very similarly, obeying the same models, such as the Kane kp model [21] that gives the basic scaling of, e.g., zone-center conduction band effective masses and optical absorption strength with bandgap energy. Hence, we expect this direct optical absorption to behave similarly to that in the direct gap semiconductors like GaAs, though with an additional, weak indirect absorption tail extending to lower photon energies.

Fig. 1(a) shows the basic structure used for our experiments. Ge quantum wells with SiGe barriers between them are grown on the top of a lattice-relaxed SiGe buffer layer on a [1 0 0]-oriented Si substrate. Because Ge has a larger lattice constant than that of Si (by about 4%), Ge grown on Si or lattice-relaxed SiGe alloys will be compressively strained. In our sample structure, we balance the strain between the wells and the barriers to get approximately zero net strain in the quantum well region (i.e., a "strain-balanced" structure); the weighted average of the silicon concentration in the Ge/SiGe quantum well layers is equal or close to that of the buffer layer. Fig. 1(b) illustrates the strain
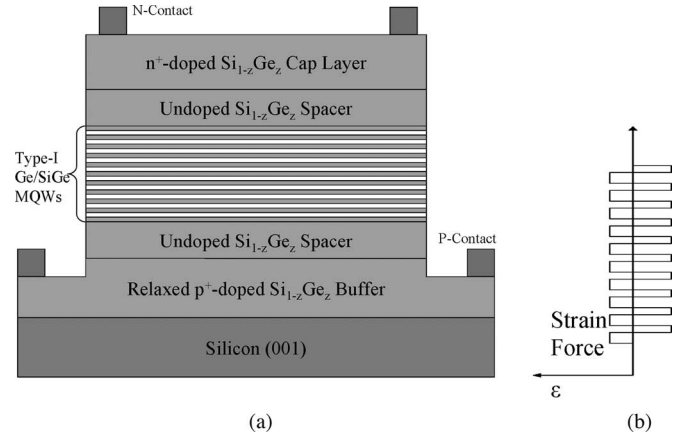

Fig. 1. (a) A p-i-n structure on silicon with Ge/Si$_{1-x}$Ge$_x$ quantum wells on relaxed Si$_{1-z}$Ge$_z$ buffer. (b) Compressive and tensile strain forces are balanced in each quantum well pair, so no strain energy is accumulated.
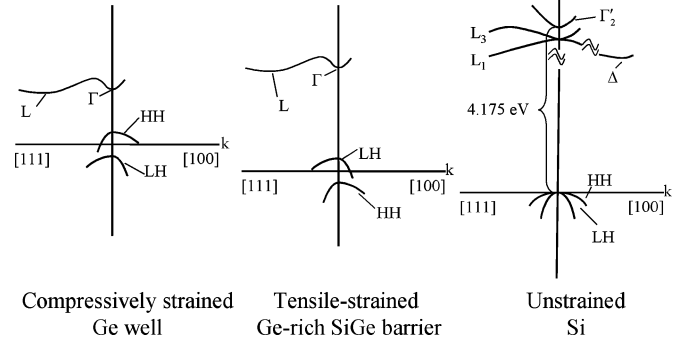

Fig. 2. Sketch of the band structure (not to scale) of the well (compressively strained Ge) and barrier (tensile-strained Ge-rich SiGe) materials, and of unstrained Si. HH: heavy hole band; LH: light hole band.

force balanced in the quantum well region. The barriers are therefore under tensile strain. The quantum wells are contained in the intrinsic region "i" of a p-i-n diode structure. Changing the voltage on the diode changes the field applied perpendicular to the quantum well layers, as required for the electroabsorption experiments. The diode structure also allows photocurrent to be collected, from which the effective optical absorption coefficient of the quantum well region can be deduced.

Fig. 2 shows the sketches of the kinds of band structures we expect in the well and barrier layers, as well as the band structure of the unstrained Si. In Fig. 2, the relevant bands are sketched along the X[1 0 0] and L[1 1 1] directions. Ge has its global conduction band minima at the L-point edges of the Brillouin zone, whereas Si's conduction band has minima at the Δ-point, within the Brillouin zone along the X-direction. Unlike much previous work on SiGe structures, all of our grown layers are Ge-like, i.e., the proportion of Ge in SiGe is very large, and the band structures of these grown layers are expected to be qualitatively more like Ge rather than like Si. (See, e.g., [22] and [23] for actual calculated Si and Ge band structures.)

Note that one effect of the strain on layers is to split the light and heavy hole bands, as indicated in Fig. 2. (The strain, and indeed the growth in a layered structure, is expected to make the light hole band somewhat heavy and the heavy hole
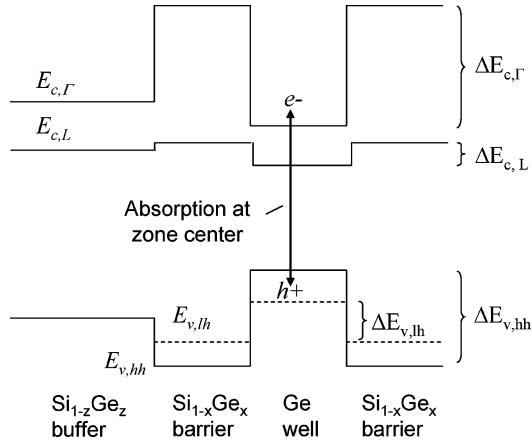
Fig. 3. Sketch of the band structure in real space (not to scale) of a Ge/SiGe quantum well structure, with compressive strain in the well and tensile strain in the barrier, on a lattice-relaxed SiGe buffer.

band somewhat light in the plane of the layers, though it should leave the hole masses in the direction perpendicular to the layers essentially at their bulk, unstrained values.)

Fig. 3 shows what we believe to be the form of the line-up of various relevant bands in a strain-balanced structure of a Ge well between SiGe barriers on a SiGe strain-relaxed substrate. We show the conduction band edge at the L-point ($E_{c,L}$) and at the Γ point ($E_{c,\Gamma}$), as well as the valence band edges corresponding to the heavy hole ($E_{v,hh}$) and light hole ($E_{v,lh}$) bands. The corresponding offsets for the conduction band at the L point ($\Delta E_{c,L}$) and the Γ point ($\Delta E_{c,\Gamma}$), and for the heavy hole ($\Delta E_{v,hh}$) and the light hole ($\Delta E_{v,lh}$) are also shown. (If the Si concentration in SiGe barriers is high enough, e.g., greater than about 15%, depending on the strain [24], the indirect minimum in the conduction can change from L to Δ.) Note that we expect type-I alignment (electron minimum energy and hole maximum energy in the same material) at the zone center, just as in typical III–V quantum well materials used for the QCSE. The specific parameters we use for various offsets and effective masses are given in Section V.

III. DEVICE FABRICATION AND EXPERIMENTAL METHODS

The SiGe quantum well structures shown in Fig. 1(a) are grown by a commercial reduced-pressure chemical vapor deposition (RPCVD) reactor. The deposition of Ge-rich SiGe or pure Ge films on Si substrates usually requires thick graded buffer layers to reduce the threading dislocation density, but this also results in a high surface roughness and needs chemical–mechanical polishing (CMP) or requires the use of a surfactant to smooth the surface [25], [26]. To obtain smooth surfaces without these smoothing techniques, several groups have made attempts to directly grow Ge on Si by different epitaxy techniques, using two growth temperature steps [27]–[29].

Here, we use direct deposition of SiGe buffers on Si instead of the graded buffer method. To control the SiGe composition in the buffer and the strain in the Ge/SiGe MQWs, a single growth temperature of $400\,°C$ is used for all layers. Si wafers [4-in, (0 0 1)-oriented, boron-doped] are used as starting substrates.

Two boron-doped (p-type) Ge-rich SiGe layers with doping levels $\sim 5 \times 10^{18}\,cm^{-3}$ are deposited on silicon. After growing the first layer, the structure is annealed at $800\,°C$ for 30–60 min. Then the second layer is deposited and the structure is annealed at $700\,°C$ for 5 min. This leaves a smooth, lattice-relaxed SiGe surface. Undoped Ge quantum wells with SiGe barriers between them are then deposited and capped by arsenic-doped (n-type) layers with doping levels $\sim 1 \times 10^{19}cm^{-3}$. Then mesas with widths from 200 to 1400 μm are patterned and plasma-etched in this grown p-i-n diode structure, opening access to the bottom p-region. Al/Ti metal rectangular rings are formed by the e-beam evaporation and lift-off and annealed for n-contacts and p-contacts.

The absorption spectra are extracted by the photocurrent measurement with different bias voltages. The light source is a quartz–tungsten–halogen bulb filtered by a 950-nm long-pass filter and a 0.25-m monochromator with a 0.4-mm slit and a 600-l/mm grating. The light is chopped and illuminated normally into the devices with random polarization. The photocurrent is measured with a lock-in amplifier. Assuming one electron of current for each absorbed photon, the responsivity is obtained by dividing the photocurrent by the light power passing through the i-region. The corresponding effective absorption coefficient is calculated based on the total thickness of the quantum wells and barriers (not just the total thickness of the Ge well material), correcting for the surface reflections.

IV. EXPERIMENTAL RESULTS

A. 10-nm Quantum Wells

Fig. 4(a) shows the absorption coefficient spectra measured at room temperature for a structure with ten Ge quantum wells, each 10-nm thick, separated by 16-nm-thick $Si_{0.15}Ge_{0.85}$ barriers, all grown on $Si_{0.1}Ge_{0.9}$ buffer layers [18]. Note first that the spectra show clear exciton absorption peaks at room temperature. In bulk Ge, an exciton absorption peak can be seen at low temperature [30], but such peaks usually are not clearly resolvable at room temperature. The appearance of room temperature peaks is characteristic of the quantum wells, and is explained by the increased confinement of the excitons [31].

At zero applied voltage, there is also a clear shift of the direct optical absorption edge from its value in bulk, unstrained Ge ($\sim$0.8 eV [20] at room temperature) to the lowest energy exciton peak position of $\sim$0.88 eV. This shift can be explained as a combination of strain and quantum confinement (see Section V for quantitative comparison). The lowest energy peak here is ascribed to the heavy hole exciton, and the second peak to the light hole exciton. The clarity of the peaks and the shift show empirically that, despite the lower energy indirect conduction bands in the wells and the barriers, there is a strong quantum confinement at the zone center in the Ge conduction and valence bands.

When an electric field is applied, there is a clear QCSE shift of the absorption edge to lower photon energies, with shifts with field that agree well with calculations [Fig. 4(b)]. Note also that the exciton peak width, $\sim$8 meV half-width at half-maximum, has little or no apparent change with applied bias. This suggests

(a)

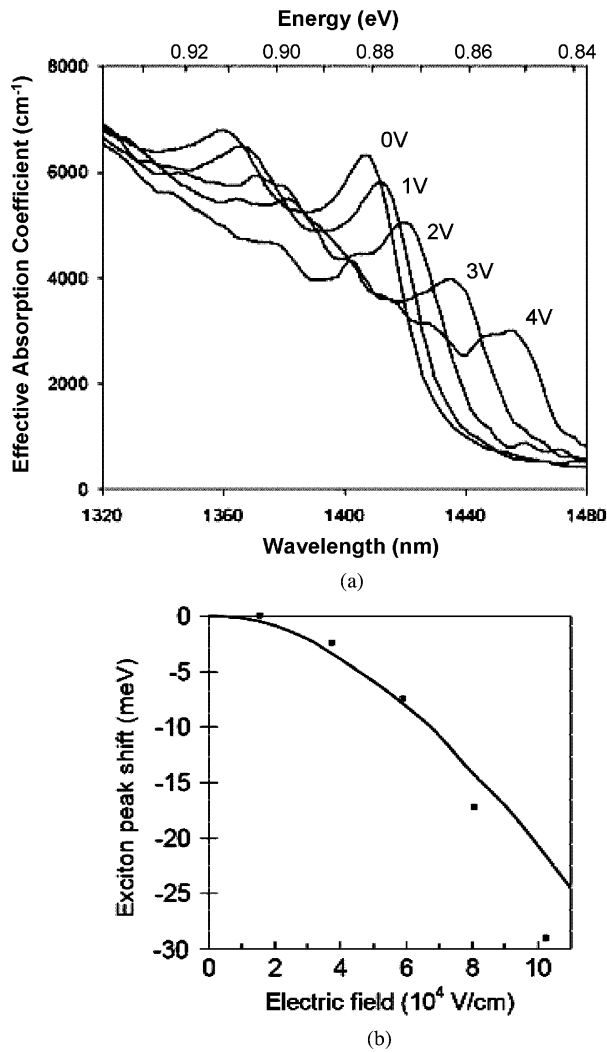(b)

Fig. 4. (a) Effective absorption coefficient spectra of Ge/SiGe (10-nm Ge well and 16-nm Ge/$Si_{0.15}Ge_{0.85}$ barrier) quantum wells on a relaxed $Si_{0.1}Ge_{0.9}$ buffer at room temperature. (b) Comparison of exciton peak shift between simulation and measurement (from [18]).

that the electric field in the i-region is relatively constant over the region, since otherwise different wells would experience different shifts, leading to a broadening of the field. This constancy in turn implies that the impurity concentration in the i-region is relatively low. This is consistent with the fact that the overall scale of the photocurrent does not depend significantly on bias over the entire voltage range, which in turn suggests that the quantum well region is fully depleted. These shifts and the exciton peaks are actually clearer, and the overall absorption coefficient, here as high as 6320 cm^{-1}, is stronger than is typically found in, for example, InGaAsP/InP quantum well structures at similar wavelengths [32].

B. 12.5-nm Quantum Wells

Though the 10-nm quantum wells show strong and clear electroabsorption, the wavelength range of operation does not match the ideal wavelengths for long-distance telecommunications, such as the C-band (~1530–1565 nm) around 1550 nm. Both
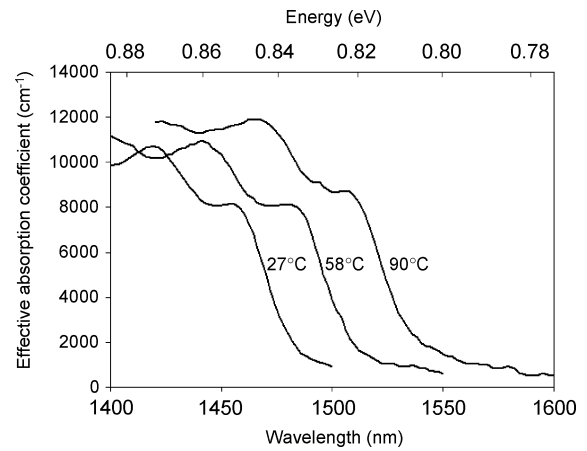

Fig. 5. Effective absorption coefficient spectra of strained Ge/SiGe (12.5-nm Ge well and 5-nm $Si_{0.175}Ge_{0.825}$ barrier) quantum wells on a relaxed $Si_{0.05}Ge_{0.95}$ buffer under 0.5-V reverse bias at different temperatures.

the quantum confinement and the compressive strain in the Ge well shift the direct absorption edge away from this wavelength range. Redesigning a quantum well with a somewhat increased thickness, and reducing the strain in the well, both help to shift the operation region back to longer wavelengths. Since the Ge direct bandgap is at ~1550 nm at room temperature, these approaches may not be enough, however, to achieve good 1550-nm operation. Increasing the quantum well thickness also eventually leads to the disappearance of the clear QCSE shift of the absorption edge with field as the electroabsorption becomes more like that in the bulk [33].

One additional way to shift the absorption to longer wavelengths is to heat the device. The direct bandgap energy in semiconductors typically reduces with increasing temperature. If the device is intended to be operated on a silicon CMOS chip, the surface of the chip may already be hot, for example, ~85 °C, under standard operating conditions in many chips. Hence, designing a modulator that runs at telecommunications wavelengths at such temperatures may actually be desirable.

Fig. 5 shows the absorption spectra at 0.5-V reverse bias at different temperatures for a structure with quantum wells made from 12.5-nm thick Ge wells and 5-nm-thick $Si_{0.175}Ge_{0.825}$ barriers on a lattice-relaxed $Si_{0.05}Ge_{0.95}$ buffer. When the device is heated up from room temperature to 90 °C, the absorption curves show a monotonic shift in the wavelength without much change in either the magnitude or the shape of the spectra. The exciton peak is still resolvable at these higher temperatures, and moves from 1456 to 1508 nm, corresponding to a temperature dependence of bandgap energy ~0.83 nm/°C (~0.47 meV/°C).

Fig. 6(a) shows the effective absorption coefficient spectra at different reverse bias voltages at 90 °C operation. The effective absorption coefficient of the exciton peak at zero bias is 9240 cm^{-1}. (This value is larger than in the 10-nm sample in part because the barriers have been chosen to be thinner here, so more quantum wells can be fitted in within a given distance.) With 0–2-V reverse bias at 90 °C, the absorption edge is shifted from ~1500 to 1560 nm by the QCSE. The effective absorption coefficient has a maximum change of 2703 cm^{-1} at 1538 nm
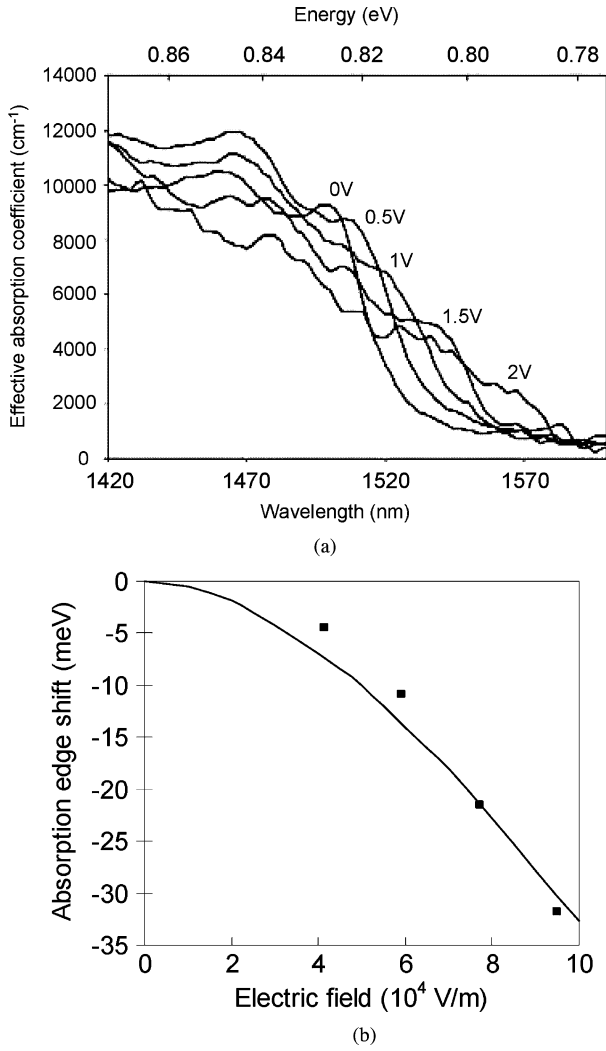
Fig. 6. (a) Effective absorption coefficient spectra of Ge/SiGe (12.5-nm Ge well and 5-nm $\mathrm{Si}_{0.175}\mathrm{Ge}_{0.825}$ barrier) quantum wells on a relaxed $\mathrm{Si}_{0.05}\mathrm{Ge}_{0.95}$ buffer under different reverse bias voltages at $90\,^{\circ}\mathrm{C}$. (b) Comparison of the electric field dependence of absorption edge shifts between the experiment and tunneling resonance simulation.

between 0- and 1.5-V bias. The peak contrast of effective absorption coefficients between 0- and 2-V bias is 3.6 at 1564 nm, and the optical bandwidth with absorption coefficient contrast higher than 3 is 20 nm.

Though the increased quantum well thickness has somewhat reduced the confinement and weakened the exciton peaks, the magnitude and shift of the QCSE are still comparable to or better than that of III–V materials at similar wavelengths. The measured shifts of the heavy-hole exciton peak shown in Fig. 6(b) agree well with the tunneling resonance simulations.

V. SIMULATIONS

The simulation of the energies of the confined electron and hole levels in the quantum wells is based on a tunneling resonance method similar to a previous work [1], [2]. In calculating QCSE shifts of the exciton peaks, in addition to the shifts of the individual electron and hole energies in the wells, there is

also some change in the exciton binding energy. We calculate this in the Appendix, though this shift with the field is so small (<0.4 meV) compared to other uncertainties that we neglect this correction in the rest of our calculations, and work only with the individual electron and hole energies and shifts.

A. Parameters for Calculations

Here, we are considering Ge and $\mathrm{Si}_{1-x}\mathrm{Ge}_x$ layers that are grown on a relaxed $\mathrm{Si}_{1-z}\mathrm{Ge}_z$ buffer layer. For such layers, we use the valence band offsets between the buffer and the layer that have been calculated by Galdin *et al.* [34, eqs. (41)–(43)] to be, for $|x - z| \leq 0.5$, and for $z > 0.5$

$$\Delta E_{\mathrm{hh}}(x, z) = [0.74 - 0.07z][x - z] \tag{1}$$

$$\begin{aligned}
\Delta E_{\mathrm{lh}}(x, z) = {} &-0.3z + 0.289z^2 - 0.142z^3 \\
&+ (0.683 - 2.58z + 3.21z^2 - 1.24z^3)x \\
&+ (0.435 + 0.704z - 2.439z^2 + 1.295z^3)x^2 \\
&+ \frac{(-0.354 - 3.77z + 8.79z^2 - 2.46z^3)}{(1 - 2.7z + 28.1z^2)}x^3.
\end{aligned} \tag{2}$$

To calculate the offsets $\Delta E_{v,\mathrm{hh}}$ and $\Delta E_{v,\mathrm{lh}}$ between the quantum well barrier and the quantum well in the valence band, one has to calculate the offset for each layer relative to the substrate, using (1), and take the appropriate difference between the two calculations.

The indirect bandgap for a strained $\mathrm{Si}_{1-x}\mathrm{Ge}_x$ layer grown on a relaxed $\mathrm{Si}_{1-z}\mathrm{Ge}_z$ buffer layer is calculated by Rieger and Vogl [24]. We do not need the numerical values here, but the result is that the lowest indirect conduction valley is expected in our structure to be in the Ge well layer, as shown in Fig. 3.

At the zone center in Si, there are several conduction bands of similar energies. The lowest conduction band at the zone center in Ge is a $\Gamma_{2'}$ band [22], and hence we consider the $\Gamma_{2'}$ band in Si [35] for calculating the conduction band offset. This $\Gamma_{2'}$ band in Si is at an energy of $\sim$4.175 eV above the top of the valence bands in pure Si. For the purposes of calculating the conduction band offset at the zone center, we make the simple assumption that this zone center bandgap varies linearly between its value in Si, and the value in bulk, unstrained Ge ($\sim$0.8 eV). Hence, subtracting the amount of the offset in the valence band, we are left with an offset in the conduction band of

$$\Delta E_{c,\Gamma} = (4.175 - 0.8)x - \Delta E_{v,\mathrm{hh}}. \tag{3}$$

As we will see later, because this is generally such a large offset, the resulting values of the quantum-confinement energies and QCSE shifts are not very sensitive to it, and so an approximate value based on simple assumptions may be sufficient, at least as a first approximation.

In our calculations, we linearly interpolate between the Ge and Si values of 0.041 and 0.156 for the $\Gamma_{2'}$ band [22] for the conduction band effective mass at the zone center and between 0.28 and 0.49 [36] for the heavy hole mass.

B. Calculations of Energy Levels and Shifts

The calculated shifts in Figs. 4(b) and 6(b) are the sums of electron and hole shifts calculated by the tunneling resonance method using the above parameters. Because of the very small calculated shift of the exciton binding energy (<0.4 meV), it is neglected in calculating shifts. (The exciton binding shift, if we were to include it, would be subtracted from these calculated shifts, slightly reducing them.)

In our strained Ge/SiGe MQWs design, we have three particularly important factors affecting the absorption edge and its QCSE shift—quantum-well thickness, barrier composition, and strain (based on buffer composition). (Barrier thickness has only a minor effect on confinement energy as long as the barrier is not too thin.) Fig. 7 illustrates the effects of each of these three factors on the quantum-confinement energies, and on the QCSE shift with fields from 0 to 11×10^4 V/cm. As is usually the case in the calculations of the QCSE shifts, the larger contribution to the shift of the transition energies is from the shift of the hole levels, because of their larger effective masses.

Fig. 7(a) shows that the quantum-well thickness is the dominant parameter (together with strain) in setting the amount of quantum-confinement energy, and hence in setting the wavelength range at which the QCSE will be observed. As is common in quantum wells, thin wells give large quantum-confinement energies, and lead to small QCSE changes in those energies. Thick wells, e.g., 15 nm or above, will show large shifts in principle, though the corresponding overlap integral between the electron and hole wavefunctions, and hence the corresponding absorption strength, will fall off very quickly with field, and the behavior will become progressively more like that of bulk materials [33].

Fig. 7(b) and (c) shows that the compositional changes in the barrier and buffer layers have only a modest effect on the quantum-confinement energies and on the QCSE shift, even though they are very important in the structural strain balance engineering for the multi-quantum-well growth.

Fig. 8 shows the effect of changing the conduction band barrier height in the simulations. A change of ± 50 meV in the conduction band barrier height causes less than ± 2-meV difference in the energy of the electron state, presumably because the electron states are well confined. Note that the calculated conduction band barrier height here is large (~ 400 meV).

For the 10-nm (and 12.5-nm) sample, the strain [24] is calculated to shift the heavy-hole-to-conduction transition energies by 36 meV (and 19 meV), and the sum of the electron and heavy hole quantum well energies from the simulation is 56 meV (and 39 meV). Adding the strain shifts and quantum-confinement shifts together, and comparing these to the actual measured positions of the exciton peaks, the calculated absolute positions are high by 12 meV (and 8 meV) respectively. Adding the effect of the exciton binding energy would reduce the calculated differences by ~ 1–2 meV (because the quantum well exciton is more tightly bound than is the bulk exciton—see the Appendix). Given the uncertainties in physical parameters, and the fact that the strain calculations have not been previously validated by comparison with experiment, the agreement
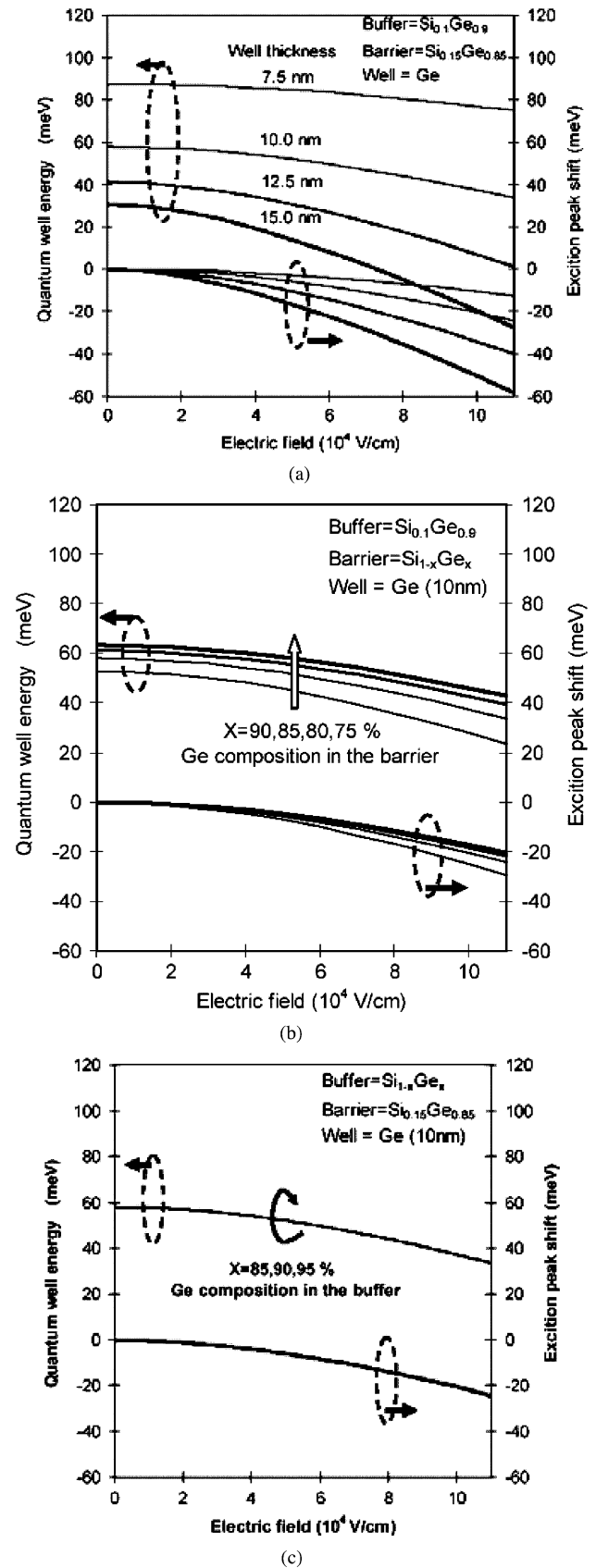

Fig. 7.   Electric field dependence of the quantum-well energy (sum of heavy hole and electron) and exciton peak shift with different structure designs. (a) Quantum-well thickness. (b) Barrier composition. (c) Buffer composition.
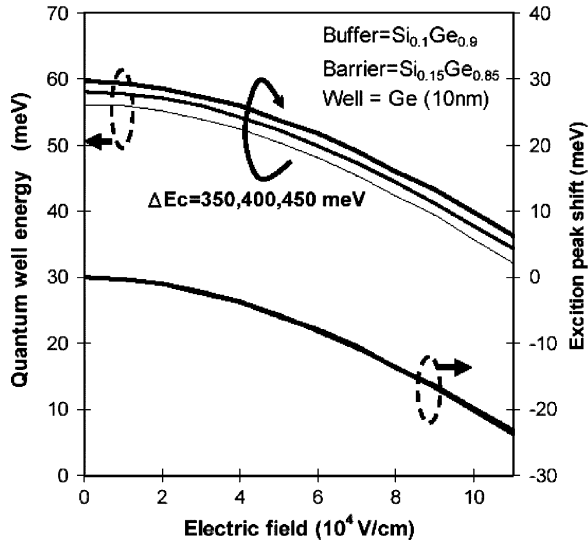
Fig. 8. Effects of variations in the direct conduction band offset on the quantum well energy with $\Delta E_c = 350, 400$, and 500 meV.

of both the absolute positions and the QCSE shifts is relatively good.

VI. DISCUSSION

Perhaps the most surprising aspect of the results presented here is that, in an indirect gap semiconductor, we can nonetheless still have strong quantum confinement at the direct gap. The electrons apparently do not leak too rapidly from the direct gap to the indirect gap.

There are at least three aspects of the experimental results that suggest we have strong quantum confinement in the direct gap quantum well.

1) Large quantum-confinement energies are required to explain the overall shift of the direct absorption edge from the bulk Ge value; the calculated strain shifts are not nearly sufficient to explain the observed shift. This shift can be explained reasonably well by the combination of the strain shifts and the quantum-well calculations using the small electron effective mass in the zone center conduction band.

2) Clear exciton peaks are observed at room temperature, which requires substantial confinement of the electron states.

3) The calculated QCSE shifts, based on the direct gap quantum well parameters, agree well with the experiments, for two different samples.

To have strong quantum-confinement effect in the optical absorption, it is not necessary that the electrons or holes stay for a long time in the states in which they are created. For example, in the GaAs quantum-well case, the exciton states themselves are known only to last for a few hundred femtoseconds [37], but that is long enough to give clear excitonic absorption lines in the spectrum. Such a short lifetime only contributes about a few millielectronvolts of the linewidth to the optical transition [31], as expected from the uncertainty principle. In Ge, the scattering time of the electrons from the Γ valley to the L valley has been measured to be ~570 fs at low temperature [38].

Though fast, this intervalley scattering time would not be fast enough to substantially broaden the optical absorption spectrum corresponding to the confined transitions.

A remaining question is whether our use of the zone-center bands to calculate the band offsets for electrons in the quantum well is valid. Such use implicitly assumes that the electrons cannot couple strongly into the L valleys in the barriers. We are not aware of any specific calculation of such coupling that would be relevant to the present cases. We can, however, attempt to rationalize that such coupling would not be strong. The side valleys, first of all, are in the L-direction, not in the [1 0 0] (X) direction of the growth and confinement in this sample, so the momentum of the electrons in such side valleys would be very different from those of the electrons in the zone-center valley. Secondly, the unit cell functions of states in those side valleys likely have different symmetry from the S-like symmetry expected in the zone-center valley. These differences in momentum and symmetry make any direct quantum-mechanical coupling between the zone-center quantum well states and the L-valley states in the barrier weak or zero. For example, if we were to consider a tight-binding model of these structures, the differences in momentum and symmetry would mean that there was little or no overlap between the zone-center well and L-valley barrier states, which would mean that the states were not directly coupled quantum mechanically. In the absence of a more detailed model, this question remains open theoretically. The experimental evidence here, though, is that the electron is confined in the zone-center valley, with relatively high effective barrier heights, at least long enough to give relatively sharp optical absorption transitions.

The fact that the electrons are expected to transfer on a picosecond or sub-picosecond time scale to the L valleys could actually be beneficial to modulator devices, because it could prevent the buildup of large electron densities in the quantum wells. Such buildup can lead to field screening and absorption saturation in modulator devices run at high-power levels. Here the electrons are expected to transfer to the L valleys, and possibly can transport relatively effectively through those L-valley states (for which the barriers are relatively low) through the whole quantum well structure.

VII. CONCLUSION

We have demonstrated clear quantum confinement at the direct gap of the Ge quantum wells with SiGe barriers, and QCSE electroabsorption in these wells. Both these effects are seen despite the fact that there are lower conduction band minima in both the well and barrier materials, confirming that the confinement of electrons in the conduction band lasts long enough to give clear quantum-confinement shifts in electron energies, and that this confinement persists even in the presence of strong electric fields. There is also a clear evidence of strong excitonic absorption peaks in the spectra, even in the presence of large electric fields, which again is consistent with the strong confinement of the electron in the conduction band zone-center quantum well. Exciton binding energy calculations confirm that the exciton is strongly confined, with a significantly increased binding energy. The absolute positions of the exciton absorption

peaks agree reasonably well with the calculated values, including the effects of both the quantum confinement and strain. The shifts of the heavy hole exciton peaks agree well with the experimental measurements.

The electroabsorption observed here is particularly interesting for possible optical modulator devices. First, it gives a strong QCSE electroabsorption mechanism in a silicon-based fabrication process, a process that is likely compatible with the standard processes used for silicon-integrated circuit manufacture. The QCSE is the mechanism used for high-performance semiconductor electroabsorption modulators, though so far only in III–V materials in practical devices. The strength of the electroabsorption in the Ge quantum wells is comparable to or better than the electroabsorption seen in III–V materials at similar wavelengths, with the exciton peaks actually more clearly defined at high fields in the present Ge case. Second, by redesigning the quantum wells with reduced strain and slightly increased thickness, we can shift the electroabsorption to longer wavelengths; when we heat the device structure to $90\,^{\circ}\mathrm{C}$, a temperature characteristic of an operating silicon-integrated circuit, the wavelength of operation of this device shifts to cover the telecommunications C-band around 1.55-μm wavelength. Hence, this mechanism with Ge quantum wells on Si may allow high-speed optical modulators compatible with both silicon-integrated circuits and optical networks.

APPENDIX

CALCULATION OF EXCITON BINDING ENERGY

We follow the variational method of [2] for calculating the exciton binding energies, except that we use electron and hole z-wavefunctions that are calculated and normalized numerically, using the tunneling resonance technique, rather than an analytic approximation to those wavefunctions.

The exciton binding energy is calculated based on the "strong confinement" assumption that the z-wavefunctions of electron and hole are approximately not perturbed by the Coulomb attraction between electron and hole. This is a good assumption if the well is relatively thin compared to the bulk exciton diameter (which it certainly is here). We therefore write the electron–hole wavefunction (with r as the relative position of the electron and hole in the xy plane) as

$$\Psi(r, z_e, z_h) = \psi_e(z_e)\psi_h(z_h)\phi_{e-h}(r) \qquad (4)$$

where $\psi_e(z_e)$ and $\psi_h(z_h)$ are the electron and hole z-wavefunctions, respectively. We use a 1S-like orbital in the xy plane, of the form

$$\phi_{e-h}(r) = \left(\frac{2}{\pi}\right)^{1/2}\frac{1}{\lambda}\exp\left(\frac{-r}{\lambda}\right) \qquad (5)$$

and we adjust the parameter λ, which we can view as the (in-plane) radius of the exciton, to minimize the energy.

For this calculation, because we should use the in-plane hole masses to calculate the exciton kinetic energy term from the in-plane orbital, we use the appropriate masses as calculated from Luttinger parameters, using values $\gamma_1 = 4.22$, $\gamma_2 = 0.39$, $\gamma_3 = 1.44$ for Si, and $\gamma_1 = 13.25$, $\gamma_2 = 4.25$, $\gamma_3 = 5.56$
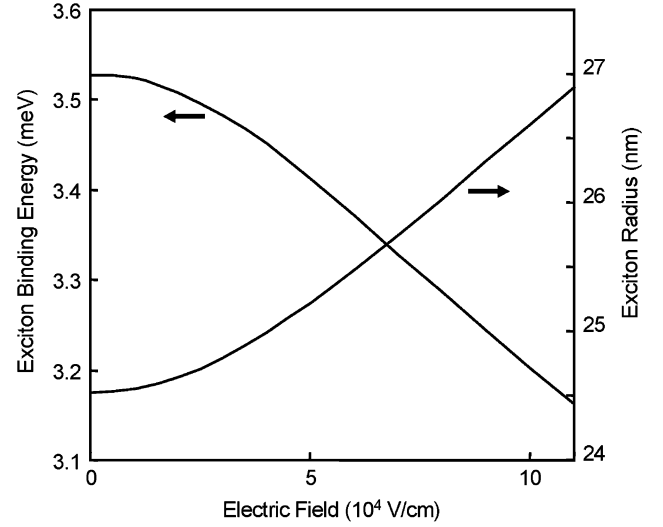

Fig. 9. Calculated exciton binding energy and exciton radius as a function of electric field perpendicular to the layers, for the 10-nm Ge quantum-well sample.

for Ge. This leads to heavy hole masses in the confinement or uniaxial strain direction, $m_{hhz} = m_0/(\gamma_1 - 2\gamma_2) \approx 0.291m_0$ for Si and $\approx 0.21m_0$ for Ge, and in the in-plane directions, $m_{hhxy} = m_0/(\gamma_1 + \gamma_2) \approx 0.216m_0$ for Si and $\approx 0.057m_0$ for Ge. For the dielectric constant, which we assume for the sake of simplicity is the same in the well and barrier layers, we use $\varepsilon_r = 16$.

The resulting exciton binding energy and exciton in-plane radius (the parameter λ) are shown in Fig. 9. For comparison, the bulk Ge exciton binding energy calculated using the effective isotropic hole mass of 0.28 used above would be $\sim$1.88 meV, with a corresponding Bohr radius for this three-dimensional (3-D) case of $\sim$23.7 nm. We see, therefore, that the effect of the confinement is to increase its binding energy; at zero field here we calculate a quantum well binding energy of $\sim$3.53 meV. The calculated two-dimensional (2-D) radius λ is actually comparable to the 3-D Bohr radius; in general, we would expect the 2-D radius to be smaller, but the fact that the hole mass used for the 2-D case is significantly lower than that used for the 3-D case increases the radius for the 2-D case. Nonetheless, with the confinement to the 10-nm thick layer, the exciton in the quantum well is substantially smaller overall, which increases the strength of the exciton absorption, and just as in, e.g., GaAs quantum wells [2], is the explanation for why the exciton peak is observable so strongly in the quantum well at room temperature. We do not have measurements at low temperature of the exciton peak form, but we also note that we do not see substantial broadening of the absorption edge or exciton peak with temperature in, e.g., Fig. 5. This lack of strong temperature dependence suggests that, in contrast to the case of GaAs quantum wells, the high-temperature width of the absorption edge or exciton peak may not be substantially caused by, e.g., the lifetime associated with the optical phonon ionization of the exciton. The source of this width in our Ge wells remains an open question; possible sources could be variations in the widths of the quantum wells (giving varying confinement energies) or rapid ionization by

the scattering of the electron, by phonon emission, to the side valleys. The fact that the exciton remains strong at high (e.g., 10^5 V/cm) fields is explicable by the presumed strong confinement of the exciton within the well by sufficiently high barriers on either side.

As the field is increased, the electron and hole are pushed to opposite sides of the well, the exciton gets somewhat larger and the exciton binding energy decreases somewhat, both because of the slightly reduced coulomb interaction of the (now more separated) electron and hole.

With the small exciton binding energy in this system, and the relatively small shift in the binding energy with field (here <0.4 meV), this shift is essentially negligible in the shift of the overall exciton peak energy, with the dominant shifts coming from the shifts in the single particle energy levels in the wells. In principle, we should include the binding energy in calculating the absolute energy positions of the transitions, though other uncertainties here (including the width of the exciton peak itself) are so large that we neglect the relatively small exciton binding energy altogether in our comparisons with experiment.

REFERENCES

[1] D. A. B. Miller, D. S. Chemla, T. C. Damen, A. C. Gossard, W. Wiegmann, T. H. Wood, and C. A. Burrus, "Band-edge electroabsorption in quantum well structures: The quantum-confined Stark effect," *Phys. Rev. Lett.*, vol. 53, no. 22, pp. 2173–2177, Nov. 1984.

[2] D. A. B. Miller, D. S. Chemla, T. C. Damen, A. C. Gossard, W. Wiegmann, T. H. Wood, and C. A. Burrus, "Electric field dependence of optical absorption near the bandgap of quantum well structures," *Phys. Rev. B*, vol. 32, no. 2, pp. 1043–1060, Jul. 1985.

[3] R. Lewen, S. Irmscher, U. Westergren, L. Thylen, and U. Eriksson, "Segmented transmission-line electroabsorption modulators," *J. Lightw. Technol.*, vol. 22, no. 1, pp. 172–179, Jan. 2004.

[4] U. Arad, E. Redmard, M. Shamay, A. Averboukh, S. Levit, and U. Efron, "Development of a large high-performance 2-D array of GaAs-AlGaAs multiple quantum-well modulators," *IEEE Photon. Technol. Lett.*, vol. 15, no. 11, pp. 1531–1533, Nov. 2003.

[5] D. A. B. Miller, "Rationale and challenges for optical interconnects to electronic chips," *Proc. IEEE*, vol. 88, no. 6, pp. 728–749, Jun. 2000.

[6] O. Kibar, D. A. Van Blerkom, C. Fan, and S. C. Esener, "Power minimization and technology comparisons for digital free-space optoelectronic interconnections," *J. Lightw. Technol.*, vol. 17, no. 4, pp. 546–555, Apr. 1999.

[7] H. Cho, P. Kapur, and K. C. Saraswat, "Power comparison between high-speed electrical and optical interconnects for interchip communication," *J. Lightw. Technol.*, vol. 22, no. 9, pp. 2021–2033, Sep. 2004.

[8] R. A. Soref, "Silicon-based optoelectronics," *Proc. IEEE*, vol. 81, no. 12, pp. 1687–1706, Dec. 1993.

[9] A. Liu, R. Jones, L. Liao, D. Samara Rubio, D. Rublin, O. Cohen, R. Nicolaescu, and M. Paniccia, "A high-speed silicon optical modulator based on a metal-oxide-semiconductor capacitor," *Nature*, vol. 427, pp. 615–618, Feb. 2004.

[10] Q. Xu, B. Schmidt, S. Pradhan, and M. Lipson, "Micrometre-scale silicon electro-optic modulator," *Nature*, vol. 435, pp. 325–327, May 2005.

[11] J. D. Cressler, "SiGe HBT technology: A new contender for Si-based RF and microwave circuit applications," *IEEE Trans. Microw. Theory Tech.*, vol. 46, no. 5, pp. 572–589, May 1998.

[12] K. W. Goossen, R. H. Yan, J. E. Cunningham, and W. Y. Jan, "Al_xGa_{1-x} As-AlAs quantum well surface-normal electroabsorption modulators operating at visible wavelengths," *Appl. Phys. Lett.*, vol. 59, no. 15, pp. 1829–1831, Oct. 1991.

[13] Y. Miyake, J. Y. Kim, Y. Shiraki, and S. Fukatsu, "Absence of Stark shift in strained $Si_{1-x}Ge_x$/Si type-I quantum wells," *Appl. Phys. Lett.*, vol. 68, no. 15, pp. 2097–2099, Apr. 1996.

[14] O. Qasaimeh, P. Bhattacharya, and E. T. Croke, "SiGe–Si quantum-well electroabsorption modulators," *IEEE Photon Technol. Lett.*, vol. 10, no. 6, pp. 807–809, Jun. 1998.

[15] C. Li, Q. Yang, H. Wang, H. Wei, J. Yu, and Q. Wang, "Observation of quantum-confined Stark shifts in SiGe/Si multiple quantum wells," *J. Appl. Phys.*, vol. 87, no. 11, pp. 8195–8197, Jun. 2000.

[16] J. S. Park, R. P. G. Karunasiri, and K. L. Wang, "Observation of large Stark shift in Ge_xSi_{1-x}/Si multiple quantum wells," *J. Vac. Sci. Technol. B*, vol. 8, no. 2, pp. 217–220, Mar. 1990.

[17] A. I. Yakimov, A. V. Dvurechenskii, A. I. Nikiforov, V. V. Ulyanov, A. G. Milekhin, A. O. Govorov, S. Schulze, and D. R. T. Zahn, "Stark effect in type-II Ge/Si quantum dots," *Phys. Rev. B*, vol. 67, no. 12, p. 125318, Mar. 2003.

[18] Y.-H. Kuo, Y. K. Lee, Y. Ge, S. Ren, J. E. Roth, T. I. Kamins, D. A. B. Miller, and J. S. Harris, "Strong quantum-confined Stark effect in germanium quantum-well structures on silicon," *Nature*, vol. 437, pp. 1334–1336, Oct. 2005.

[19] G. G. MacFarlane, T. P. McLean, J. E. Quarrington, and V. Roberts, "Fine structure in the absorption-edge spectrum of Ge," *Phys. Rev.*, vol. 108, no. 6, pp. 1377–1383, Dec. 1957.

[20] W. C. Dash and R. Newman, "Intrinsic optical absorption in single-crystal germanium and silicon at 77°K and 300°K," *Phys. Rev.*, vol. 99, no. 4, pp. 1151–1155, Aug. 1955.

[21] E. O. Kane, "Band structure of indium antimonide," *J. Phys. Chem. Solids*, vol. 1, pp. 249–261, 1957.

[22] M. Cardona and F. H. Pollak, "Energy-band structure of germanium and silicon: The kp method," *Phys. Rev.*, vol. 142, no. 2, pp. 530–543, Feb. 1996.

[23] J. R. Chelikovsky and M. L. Cohen, "Nonlocal pseudopotential calculation for the electronic structure of eleven diamond and zinc-blende semiconductors," *Phys. Rev. B*, vol. 14, no. 2, pp. 556–582, Jul. 1976.

[24] M. M. Rieger and P. Vogl, "Electronic-band parameters in strained $Si_{1-x}Ge_x$ alloys on $Si_{1-y}Ge_y$ substrates," *Phys. Rev. B*, vol. 48, no. 19, pp. 14276–14287, Nov. 1993.

[25] M. T. Currie, S. B. Samavedam, T. A. Langdo, C. W. Leitz, and E. A. Fitzgerald, "Controlling threading dislocation densities in Ge on Si using graded SiGe layers and chemical-mechanical polishing," *Appl. Phys. Lett.*, vol. 72, no. 14, pp. 1718–1720, Apr. 1998.

[26] J. L. Liu, S. Tong, Y. H. Luo, J. Wan, and K. L. Wang, "High-quality Ge films on Si substrates using Sb surfactant-mediated graded SiGe buffers," *Appl. Phys. Lett.*, vol. 79, no. 21, pp. 3432–3434, Nov. 2001.

[27] H.-C. Luan, D. R. Lim, K. K. Lee, K. M. Chen, J. G. Sandland, K. Wada, and L. C. Kimerling, "High-quality Ge epilayers on Si with low threading-dislocation densities," *Appl. Phys. Lett.*, vol. 75, no. 19, pp. 2909–2911, Nov. 1999.

[28] Y.-H. Kuo, X. Yu, J. Fu, T. I. Kamins, G. S. Solomon, and J. S. Harris, "Direct growth of Ge on Si by molecular beam epitaxy for CMOS integrated long wavelength optical devices," presented at the Mater. Res. Soc. Spring Meeting, Symp. D1.9, San Francisco, CA, Mar. 2005.

[29] O. O. Olubuyide, D. T. Danielson, L. C. Kimerling, and J. L. Hoyt, "Impact of seed layer on material quality of epitaxial germanium on silicon deposited by low pressure chemical vapor deposition," presented at the 4th Int. Conf. Silicon Epitaxy Heterostruct. (ICSI-4), Sec. B3, Hyogo, Japan, May 2005.

[30] H. Schweizer, A. Forchel, A. Hangleiter, S. Schmitt Rink, J. P. Löwenau, and H. Haug, "Ionization of the direct-gap exciton in photoexcited germanium," *Phys. Rev. Lett.*, vol. 51, no. 8, pp. 698–701, Aug. 1983.

[31] D. S. Chemla, D. A. B. Miller, P. W. Smith, A. C. Gossard, and W. Wiegmann, "Room temperature excitonic nonlinear absorption and refraction in GaAs/AlGaAs multiple quantum well structures," *IEEE J. Quantum Electron.*, vol. 20, no. 3, pp. 265–275, Mar. 1984.

[32] N. C. Helman, J. E. Roth, D. P. Bour, H. Altug, and D. A. B. Miller, "Misalignment-tolerant surface-normal low-voltage modulator for optical interconnects," *IEEE J. Sel. Topics Quantum Electron.*, vol. 11, no. 2, pp. 338–342, Mar.–Apr. 2005.

[33] D. A. B. Miller, D. S. Chemla, and S. Schmitt Rink, "Relation between electroabsorption in bulk semiconductors and in quantum wells: The

quantum-confined Franz–Keldysh effect," *Phys. Rev. B*, vol. 33, no. 10, pp. 6976–6982, May 1986.

[34] S. Galdin, P. Dollfus, V. Aubry Fortuna, P. Hesto, and H. J. Osten, "Band offset predictions for strained group IV alloys: $Si_{1-x-y}Ge_xC_y$ on $Si(0\,0\,1)$ and $Si_{1-x}Ge_x$ on $Si_{1-z}Ge_z(001)$," *Semicond. Sci. Technol.*, vol. 15, no. 6, pp. 565–572, Jun. 2000.

[35] T. Ebner, K. Thonke, R. Sauer, F. Schaeffler, and H. J. Herzog, "Electroreflectance spectroscopy of strained $Si_{1-x}Ge_x$ layers on silicon," *Phys. Rev. B*, vol. 57, no. 24, pp. 15448–15453, Jun. 1998.

[36] S. M. Sze, *Physics of Semiconductor Devices*, 2nd ed. New York: Wiley, 1981, p. 850.

[37] W. H. Knox, R. L. Fork, M. C. Downer, D. A. B. Miller, D. S. Chemla, C. V. Shank, A. C. Gossard, and W. Wiegmann, "Femtosecond dynamics of resonantly excited excitons in room temperature GaAs quantum wells," *Phys. Rev. Lett.*, vol. 54, no. 12, pp. 1306–1309, Mar. 1985.

[38] G. Mak and W. W. Rühle, "Femtosecond carrier dynamics in Ge measured by a luminescence up-conversion technique and near-band-edge infrared excitation," *Phys, Rev. B*, vol. 52, no. 16, pp. R11584–R11587, Oct. 1995.

Yu-Hsuan Kuo (S'05) received the B.S. degree in electrophysics from the National Chiao Tung University, Hsinchu, Taiwan, R.O.C., in 2000. He received the M.S. and Ph.D. degrees from Stanford University, Stanford, CA, in 2003 and 2006, respectively, both in electrical engineering.

Currently, he is with the Solid State and Photonics Laboratory, Stanford University. His current research interests include silicon photonics and quantum electronics for high-speed interconnects.

Yong Kyu Lee (M'05) received the B.S. and M.S. degrees from Korea University, Seoul, Korea, in 1993 and 1995, respectively, both in materials science and engineering. He received the Ph.D. degree in electronics engineering from Seoul National University, Seoul, in 2004.

From 1995 to 2001, he was with Samsung Electronics, Kyungsangbuk-do, Korea, where he contributed to the development of advanced EEPROM and flash memories and their characterizations. From 2001 to 2004, he was with the Semiconductor Materials and Devices Laboratory (SMDL), Seoul National University, where he worked on the nanoscaled multilevel (bit) SONOS-type flash memories. From 2004 to 2005, he was a Postdoctoral Fellow at Stanford University, Stanford, CA, where he worked on strong QCSE in germanium quantum-well structures on silicon. In 2006, he joined Samsung Electronics again. His current research interests include nano-CMOS devices and new nonvolatile memories (NVMs).

Yangsi Ge received the B.S. degree in fundamental sciences from Tsinghua University, Beijing, China, in 2003. He is currently working toward the Ph.D. degree in applied physics at Stanford University, Stanford, CA.

His current research interests include optical interconnects based on silicon photonics.

Shen Ren received the B.S. degree from Peking University, Beijing, China, in 2004, and the M.S degree from Stanford University, Stanford, CA, in 2006, both in electrical engineering. He is currently working toward the Ph.D. degree in electrical engineering at Stanford University.

His current research interests include optical interconnects based on silicon photonics.

Jonathan E. Roth received the B.S. degree in biomedical engineering from Case Western Reserve University, Cleveland, OH, in 2000. He is currently working toward the Ph.D. degree in electrical engineering at Stanford University, Stanford, CA.

From 2000 to 2001, he was a Fulbright Scholar at Lund Institute of Technology, where he worked on tissue optics and photodynamic therapy. His current research interests include optoelectronic modulators for optical interconnects.

Theodore I. (Ted) Kamins (S'65–M'68–SM'79–F'91) received the B.S., M.S., and Ph.D. degrees from the University of California, Berkeley, all in electrical engineering.

He is currently a Principal Scientist in the Quantum Science Research Group, Hewlett-Packard Laboratories, Palo Alto, CA, where he has conducted research on numerous semiconductor material and device topics. He is also a Consulting Professor in the Electrical Engineering Department, Solid State and Photonics Laboratory, Stanford University, Stanford, CA. He has also worked on epitaxial and polycrystalline silicon at the Research and Development Laboratory of Fairchild Semiconductor. His current research interests include advanced nanostructured electronic materials and devices. He is the author of *Polycrystalline Silicon for Integrated Circuits and Displays* (Kluwer, 1998), and a coauthor of *Device Electronics for Integrated Circuits* (Wiley, 2003).

Dr. Kamins is a Fellow of the Electrochemical Society.

David A. B. Miller (M'84–SM'89–F'95) received the B.Sc. degree in physics from St. Andrews University, Fife, U.K., and the Ph.D. degree in physics from Heriot-Watt University, Edinburgh, UK, in 1979.

From 1981 to 1996, he was with Bell Laboratories, where he was a Department Head from 1987, latterly of the Advanced Photonics Research Department. He is currently the W. M. Keck Professor of Electrical Engineering at Stanford University, Stanford, CA, and the Director of the Ginzton and Solid State and Photonics Laboratories, Stanford University. His current research interests include quantum-well optoelectronic and nanophotonic physics and devices, and fundamental and applications of optics in information, sensing, switching, and processing. He is the author or coauthor of more than 250 scientific papers. He is the holder of 60 patents.

Dr. Miller has served as a Board Member for both the Optical Society of America (OSA) and the IEEE Lasers and Electro-Optics Society (LEOS), and in various other society and conference committees. He was the President of the IEEE LEOS in 1995. He is the recipient of the Adolph Lomb Medal and the R. W. Wood Prize from the OSA, the International Prize in Optics from the International Commission for Optics, and the IEEE Third Millennium Medal. He is a Fellow of the Royal Societies of London and Edinburgh, OSA, and American Physical Society (APS), and holds honorary degrees from the Vrije Universiteit Brussel and Heriot-Watt University.

James S. Harris, Jr. (S'65–M'69–SM'78–F'88) received the B.S., M.S., and Ph.D. degrees from Stanford University, Stanford, CA, in 1964, 1965, and 1969, respectively, all in electrical engineering.

In 1969, he joined the Rockwell International Science Center, Thousand Oaks, CA, where he was one of the key contributors in developing their preeminent position in GaAs device technology. In 1982, he joined the Solid State Electronics Laboratory, Stanford University, as a Professor of electrical engineering. From 1984 to 1998 and from 1985 to 1999, respectively, he served as a Director of the Solid State Electronics Laboratory and the Joint Services Electronics Program, Stanford University. He is currently the James and Ellenor Chesebrough Professor of Engineering at Stanford University. He has supervised over 85 Ph.D. students. He is the author or coauthor of more than 750 publications. He is the holder of 18 U.S. patents. His current research interests include the physics and application of ultrasmall structures and novel materials to new high-speed and spin-based electronic and optoelectronic devices and systems.

Dr. Harris is a Fellow of the American Physical Society and Optical Society of America. He is the recipient of the 2000 IEEE Morris N. Liebmann Memorial Award, 2000 International Compound Semiconductor Conference Walker Medal, IEEE Third Millennium Medal, and Alexander von Humboldt Senior Research Prize in 1998 for his contributions to GaAs devices and technology.